Structure of Mixed Anionic/Nonionic Surfactant Micelles: Experimental Observations Relating to the Role of Headgroup Electrostatic and Steric Effects and the Effects of Added Electrolyte

J. Penfold,*,† I. Tucker,‡ R. K. Thomas,§ E. Staples,† and R. Schuermann||

ISIS Facility, Rutherford Appleton Laboratory, Chilton, Didcot, OXON, U.K., Unilever Research and Development, Port Sunlight, Quarry Road East, Bebington, Wirral, U.K., Physical and Theoretical Chemistry Department, Oxford University, South Parks Road, Oxford, U.K., and Paul Scherrer Institute, 5232 Villigen PSI, Switzerland

Received: February 10, 2005; In Final Form: April 1, 2005

The structures of the mixed anionic/nonionic surfactant micelles of SDS/$C_{12}E_6$ and SDS/$C_{12}E_8$ have been measured by small angle neutron scattering (SANS). The variations in the micelle aggregation number and surface charge with composition, measured in D_2O and in dilute electrolyte, 0.01 and 0.05 M NaCl, provide data on the relative roles of the surfactant headgroup steric and electrostatic interactions and their contributions to the free energy of micellization. For the SDS/$C_{12}E_8$ mixture, solutions increasingly rich in $C_{12}E_8$ show a modest micellar growth and an increase in the surface charge. The changes with increasing electrolyte concentration are similarly modest. In contrast, for the SDS/$C_{12}E_6$ mixture, solutions rich in $C_{12}E_6$ show a more significant increase in aggregation number. Furthermore, electrolyte has a more substantial effect on the aggregation for the nonionic ($C_{12}E_6$) rich mixtures. The experimental results are discussed in the context of estimates of the steric and electrostatic contributions to the free energy of micellization, calculated from the molecular thermodynamic approach. The variation in micelle surface charge is discussed in the context of the "dressed micelle" theory for micelle ionization, and other related data.

1. Introduction

The study of surfactant mixing in micelles and at interfaces is of considerable current interest for both theoretical and practical reasons.[1,2] The widespread use of surfactants in the many practical applications such as detergency usually involves mixtures because they provide synergistic enhancements of many aspects of performance and behavior and because commercially used surfactants are often inherent mixtures. Although there is a rich background of information on surfactant mixing from classical measurements such as surface tension[3] and thermodynamic treatments based on the pseudophase approximation,[4,5] many aspects of surfactant mixing are still relatively poorly understood. Developing a more detailed understanding of surfactant mixing, in micelles and at interfaces, remains an important issue. The development of new theoretical treatments and experimental methods has resulted in a resurgence of interest and activity in the area.[6,7]

The molecular thermodynamic theories of surfactant micellization[8,9] are one of those new approaches and are developments of the simpler, but highly effective geometrical "packing" approaches of Tanford[10] and Israelachivili, Mitchell, and Ninham.[11] Their extension to mixed micellization[12−16] has, in recent years, been an important growth area in the development of theories of surfactant mixing. Although the regular solution theory,[4,5] in which the departure from ideal mixing is characterized by a single interaction parameter, β, has been highly successfully applied, the molecular thermodynamic approach in principle provides the opportunity to obtain a greater physical insight. In particular, it now provides experimentalists with the opportunity to consider in more detail the different contributions to the free energy of micellization and how they are affected by the specific molecular nature of the different mixed components. Furthermore, the same basic approach has now been applied to describe surfactant mixing at interfaces.[17,18]

In parallel with these theoretical developments, in the last two decades, new experimental methodologies, which include neutron and X-ray small angle scattering,[19,20] light scattering,[21] fluorescence,[22] NMR,[23] and cryo-TEM,[24] have been developed to provide more detailed and more precise information on micelle size, shape, dynamics, and, especially for mixtures, micelle composition.

In the recent literature, a wide range of different surfactant mixtures has been studied, using a variety of different experimental approaches, and includes nonionic mixtures,[25] ionic mixtures,[26] and mixtures of ionic and nonionic surfactants with zwitterionic[27] and Gemini[28] surfactants. In the context of this paper, and in the context of the mixtures that are of most practical importance, some of the recent studies on ionic/nonionic surfactant mixtures are cited here. Griffiths et al.[29,30] have used NMR, electron paramagnetic resonance (EPR), and small angle neutron scattering (SANS) to investigate the nature of sodium dodecyl sulfate (SDS)/sugar based nonionic surfactant mixed micelles, and Bucci et al.[31] used SANS to investigate the related mixture of SDS/β-dodecyl maltoside. Fluorescence and SANS have been used to investigate the nonionic/cationic surfactant mixtures of Triton X100/bromo-4-tridecylpyridine[32] and Triton X100/alkylammonium bromide.[33] Other SDS/nonionic surfactant mixtures have included the use of SANS and

† Rutherford Appleton Laboratory.
‡ Unilever Research and Development.
§ Oxford University.
|| Paul Scherrer Institute.

10.1021/jp050727f CCC: $30.25
Published on Web 05/03/2005

light scattering to study sodium dodecyl sulfonate/$C_{12}E_6$,[34] ESR to study SDS/$C_{12}E_6$ and DTAC/$C_{12}E_6$,[35] NMR to study sodium hexasulfonate/C_6E_5[36] and SDS/Brij-35 (CTAB/Brij-35),[37] and SANS to study SDS/$C_{12}E_4$.[38] A number of recent studies have focused on the anionic/nonionic mixture of SDS/$C_{12}E_6$,[35,39−43] which is the subject of this paper.

Small angle neutron scattering (SANS), in combination with H/D isotopic substitution, provides the opportunity to measure both structure and composition in mixed surfactant micelles.[19,39] Although extensively used to measure micelle structure in single surfactant systems,[19] its application to mixed micelles is relatively recent. This was the focus of the work by Penfold et al.[40,41] on SDS/$C_{12}E_6$ mixtures, where the emphasis was on evaluating the variation in micelle composition and size in the context of regular solution theory (RST) for solutions relatively rich in SDS and with added electrolyte. In a similar concentration and electrolyte regime, Blankschtein et al.[42] used light scattering to follow micellar growth for solutions rich in nonionic surfactant, where the observation of a maximum in the aggregation number with composition was rationalized in terms of the surfactant headgroup electrostatic and steric contributions to the free energy of micellization. A qualitatively similar observation was subsequently reported by Penfold et al.[41] for SDS/$C_{12}E_6$ from SANS measurements. More recently, Garamus[43] has reinvestigated the SDS/$C_{12}E_6$ mixture in the absence of electrolyte and at temperatures below room temperature, in an attempt to clarify further the relative contributions of the headgroup steric and electrostatic interactions to the free energy of micellization.

The aim of this study is to clarify the roles of the headgroup steric and electrostatic contributions to the free energy of micellization, where the steric contribution is manipulated by using EO_6 and EO_8 nonionic headgroups and the electrostatic contribution is altered by solution composition (measurements were made over a range of compositions from anionic to nonionic rich) and the addition of relatively low electrolyte concentrations. In this paper, we have used SANS to investigate the mixed surfactant micelles of SDS/$C_{12}E_6$ and SDS/$C_{12}E_8$ in D_2O and in weak electrolyte (0.01 and 0.05 M NaCl).

2. Experimental Details

The SANS measurements were made on the LOQ diffractometer[44] at the ISIS pulsed neutron source at the Rutherford Appleton Laboratory. The measurements were made using the white beam time-of-flight method, in the scattering vector range from 0.008 to 0.25 $Å^{-1}$. The samples were contained in Hellma 1 mm path length quartz spectrophotometer cells and maintained at a temperature of 25 °C. The data were corrected for background scattering, detector response, and the spectral distribution of the incident neutron beam and converted to an absolute scattering cross section ($I(Q)$, in cm^{-1}) using standard procedures.[44]

Measurements were made for the anionic/nonionic surfactant mixtures of SDS/$C_{12}E_6$ and SDS/$C_{12}E_8$ at a solution concentration of 25 mM D_2O and 0.01 and 0.05 M NaCl. The measurements for SDS/$C_{12}E_6$/D_2O were made in the composition range from 10/90 to 80/20 mole ratio and in 0.01 and 0.05 M NaCl in the composition range from 3/97 to 70/30 mole ratio. For all these measurements, the isotopic combination of *h*-SDS/*h*-$C_{12}E_6$ was used. For the surfactant combination of SDS/$C_{12}E_8$, the measurements were made in D_2O and 0.01 and 0.05 M NaCl in the composition range from 10/90 to 80/20 mole ratio. In 0.01 and 0.05 M NaCl, the isotopic combination of *h*-SDS/*h*-$C_{12}E_8$/D_2O was used, and for the measurements in D_2O (in the absence of electrolyte), the isotopic combinations *h*-SDS/*h*-$C_{12}E_8$/D_2O and *d*-SDS/*h*-$C_{12}E_8$/D_2O were measured (where *d*-SDS refers to the alkyl chain deuterium labeled).

The protonated surfactants were obtained from Nikkol (*h*-$C_{12}E_6$, *h*-$C_{12}E_8$) and were used as supplied. The *h*-SDS was obtained from Polysciences. The deuterium labeled SDS (*d*-SDS) was synthesized, purified, and characterized using methods described elsewhere.[46] The *h*-SDS was subjected to the same purification and characterization protocol as the *d*-SDS. The chemical purities of all the surfactants were assessed by surface tension or TLC and were found to be sufficiently pure to use at the solution concentration (25 mM) without complicating the data interpretation. Deuterium oxide (D_2O) was supplied by Fluorochem, and high purity water (Elga Ultrapure) was used throughout. All glassware and sample cells were cleaned using alkali detergent (Decon 90), followed by copious washing in high purity water.

In SANS, the scattering cross section, or scattered intensity, for colloidal aggregates in solution can be written by the general expression[47]

$$I(Q) = N|\int_v(\rho_p(r) - \rho_s)\exp iQr\, d^3r|^2 \quad (1)$$

where ρ_p and ρ_s are the aggregate and solvent scattering length densities and N is the number of aggregates per unit volume.

In the micellar phase, the micelle structure is determined by analyzing the scattering data using a standard and well-established model for globular micelles.[46] For a solution of globular polydisperse interacting particles (micelles), the scattered intensity can be written, in the "decoupling approximation"[47] as

$$I(Q) = n[S(Q)|\langle F(Q)\rangle_Q|^2 + \langle|F(Q)|^2\rangle_Q - |\langle F(Q)\rangle_Q|^2] \quad (2)$$

where the averages denoted by $\langle Q\rangle$ are averages over particle size and orientation, n is the micelle number density, $S(Q)$ is the structure factor, and $F(Q)$ is the form factor. The micelle structure (form factor) is modeled using a standard "core and shell" model,[47] where the form factor is

$$F(Q) = V_1(\rho_1 - \rho_2)F_0(QR_1) + V_2(\rho_2 - \rho_s)F_0(QR_2) \quad (3)$$

and R_1 and R_2 are the core and shell radii, $V_i = 4\pi R_i^3/3$, $F_0(QR_i) = 3j_1(QR_i)/(QR) = 3[\sin(QR) - QR\cos(QR)]/(QR)^3$, ρ_1, ρ_2, and ρ_s are the scattering length densities of the micelle core, the micelle shell, and the solvent, and $j_1(QR_i)$ is a first-order spherical Bessel function.

The micelle core + shell model[47] comprises an inner core made up of the alkyl chains only and constrained to space fill a volume limited by a radius, R_1, the fully extended chain length of the surfactant (l_c). For larger aggregation numbers (ν), volumes greater than that defined by R_1 (as is found in this study) are accommodated by a prolate elliptical distortion with dimensions R_1, R_1, eR_1 (where e is the elliptical ratio). The outer shell, of dimensions R_2, R_2, eR_2, contains headgroups and the corresponding hydration water. Representative hydration values for the EO headgroup, the cation, and the bound counterions are included as fixed values,[47] and the modeling is not particularly sensitive to variations in hydration.[50] The packing constraints include the measured or assumed micelle composition (see later discussion). From the known molecular volumes and neutron scattering lengths, the scattering length density (ρ) for the core, shell, and solvent can be estimated.[47] The interparticle interactions are included using the rescaled mean spherical approximation (RMSA), calculated for a repulsive

TABLE 1: cmc Values for SDS, $C_{12}E_6$, and $C_{12}E_8$

	cmc ($\times 10^{-3}$ M)		
surfactant	in D_2O	in 0.01 M NaCl	in 0.05 M NaCl
SDS	8	5	3
$C_{12}E_6$	8.7×10^{-2}		
$C_{12}E_8$	9×10^{-2}		

TABLE 2: Model Parameters for SDS/$C_{12}E_6$ Mixed Micelles at a Concentration of 25 mM[a]

solution composition (mole % SDS)	ν	z	R_2 (Å)	e	f
		(a) In D_2O			
10/90	141	9.8	22.6	2.37	0.94
20/80	116	14.4	22.4	1.95	0.98
30/70	104	16.9	22.2	1.74	1.0
40/60	98	18.0	22.0	1.63	1.04
50/50	89	19.3	21.8	1.5	1.04
60/40	86	19.9	21.5	1.45	1.03
70/30	81	19.1	21.2	1.36	1.03
80/20	77	18.1	20.8	1.3	0.97
		(b) In 0.01 M NaCl			
3/97	402	0.0	22.7	6.74	0.92
5/95	303	7.1	22.6	5.09	0.98
10/90	179	10.5	22.5	3.0	0.99
15/85	140	14.7	22.3	2.35	0.99
20/80	129	16.5	22.2	2.16	1.03
25/75	125	18.4	22.1	2.1	1.03
30/70	119	20.8	21.9	2.0	1.02
50/50	106	23.7	21.3	1.77	0.95
70/30	101	23.2	20.7	1.7	0.97
		(c) In 0.05 M NaCl			
3/97	396	0.0	22.7	6.6	0.94
5/95	480	0.0	22.6	8.08	0.94
10/90	362	0.0	22.5	6.1	0.94
15/85	229	10.8	22.3	3.72	0.9
20/80	159	12.0	22.2	2.66	0.91
25/75	141	19.7	22.1	2.37	0.9
30/70	134	25.2	21.9	2.25	0.9
50/50	120	32.6	21.3	2.02	0.91
70/30	116	31.6	20.7	1.95	1.0

[a] In part a, κ varied over the composition range from 0.0094 to 0.028 Å^{-1} and $R_1 = 16.7$ Å; in part b, κ varied over the composition range from 0.033 to 0.042 Å^{-1}; and in part c, κ varied over the composition range from 0.072 to 0.075 Å^{-1}.

screened Coulombic potential,[48,49] defined by the surface charge (z), the micelle number density (n), the micelle diameter, and the Debye−Huckel inverse screening length (κ).[48] The model parameters refined are then ν, z, and e, and an acceptable model fit requires the shape of the scattering to be reproduced and the absolute value of the scattered intensity to be predicted to within ±10%. The scale factor (f), the ratio of the measured intensity to the model calculated value, shows the variation in the absolute scaling of the data fits (see Tables 1 and 3). The values of the aggregation numbers obtained confirm using simple packing arguments[11] that ellipsoids rather than polydisperse spheres are an appropriate model.[8]

For the data where two isotopic combinations, *h*-ionic/*h*-nonionic and *d*-ionic/*h*-nonionic (*hh*, *dh*), were measured, the ratio of the two scattered intensities extrapolated to small Q gives an estimate of the micelle composition (mole fraction of each surfactant component),[39] as has been demonstrated for a range of micellar systems.[39−41] In the limit of small Q and for dilute systems (where $S(Q)$, $P(Q) \sim 1.0$), the scattered intensity is approximately

$$I(Q) \approx \sum_i N_i V_i^2 (\rho_{ip} - \rho_s)^2 \qquad (4)$$

TABLE 3: SDS/$C_{12}E_6$ Mixed Micelles: Degree of Ionization

solution composition (mole % SDS)	in D_2O		in 0.01 M NaCl		in 0.05 M NaCl	
	δ	δ(per SDS)	δ	δ(per SDS)	δ	δ(per SDS)
3/97			0.0	0.0	0.0	0.0
5/95			0.02	0.47	0.0	0.0
10/90	0.07	0.7	0.06	0.58	0.0	0.0
15/85			0.11	0.7	0.05	0.32
20/80	0.12	0.62	0.13	0.63	0.08	0.38
25/75			0.15	0.59	0.14	0.56
30/70	0.16	0.54	0.17	0.60	0.19	0.63
40/60	0.18	0.46				
50/50	0.22	0.43	0.22	0.45	0.27	0.54
60/40	0.23	0.38				
70/30	0.24	0.34	0.23	0.33	0.27	0.39
80/20	0.24	0.20				

where N is the micelle number density, V is the micelle "dry" volume, ρ_{ip} is the micelle scattering length density, ρ_s is the solvent scattering length density, and $\sum_i$ is over all micelle compositions for a binary mixture of surfactants. Changing the isotopic labeling of one of the surfactant components changes ρ_{ip}, so a simple ratio of the intensities for the two different isotopic combinations provides directly an estimate of the volume (mole) fraction of the two components. Although eq 4 is strictly valid only for dilute solutions, it is applicable to more concentrated solutions provided that $S(Q)$ and $P(Q)$ do not change substantially with isotopic labeling.[39]

Equation 4 was used, as previously described,[39] to evaluate the micelle composition for the SDS/$C_{12}E_8$ mixture in D_2O. Consistent with previous observations for SDS/$C_{12}E_6$[39−41] and the predictions of RST, at a solution concentration of 25 mM (which is at least 50 times the critical micelle concentration (cmc) at the highest levels of SDS measured), the micelle composition is close to the solution composition. In the subsequent model analysis of the micellar scattering data (using eqs 2 and 3 and the core + shell model described), the micelle composition is fixed at the solution composition. The Debye−Huckel inverse screening length (κ) is calculated from the estimated monomer concentration and (in the case of added electrolyte) the electrolyte concentration. The micelle number density (n) (and micelle volume fraction (ϕ)) is calculated from the known surfactant concentration, the cmc, and the solution concentration such that

$$n = cN/v \qquad (5)$$

where c is the micelle concentration ($c = c_s - \text{cmc}$, where c_s is the solution concentration), and the volume fraction of micelles is

$$\phi = NcV/v \qquad (6)$$

where V is the micelle volume. The cmc values for SDS, $C_{12}E_6$, and $C_{12}E_8$ can be found in Table 1.

3. Results

3.1. SDS/$C_{12}E_6$. Figure 1 shows the small angle neutron scattering data for 25 mM *h*-SDS/*h*-$C_{12}E_6$ in D_2O (Figure 1a), in 0.01 M NaCl (Figure 1b), and in 0.05 M NaCl (Figure 1c). The scattering in D_2O, in the absence of electrolyte (Figure 1a), is consistent with the expected behavior for globular interacting micelles. The peak in the scattering patterns, associated with the intermicellar interactions, shifts systematically to lower Q values for solutions progressively rich in the nonionic surfactant $C_{12}E_6$, consistent with micellar growth. However, the scattering patterns (over the entire composition range measured) remain

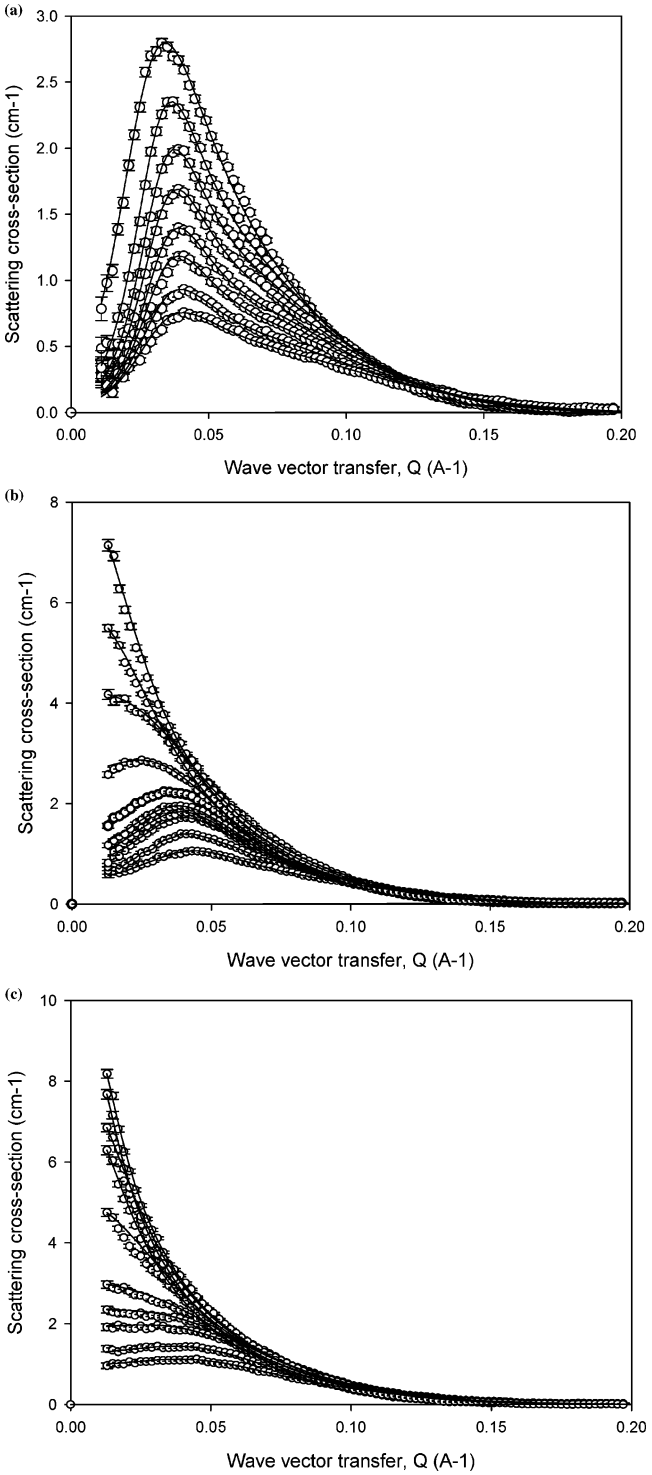

Figure 1. Scattered intensity for 25 mM *h*-SDS/*h*-$C_{12}E_6$ (a) in D_2O, (b) in 0.01 M NaCl, and (c) in 0.05 M NaCl for different SDS/$C_{12}E_6$ solution compositions: (a) from bottom curve to top curve, 80/20, 70/30, 60/40, 50/50, 40/60, 30/70, 20/80, and 10/90; (b) from bottom curve to top curve, 70/30, 50/50, 30/70, 25/75, 20/80, 15/85, 10/90, 5/95, and 3/97; (c) same as part b. The solid lines are model calculations as described in the text and using the parameters in Table 1.

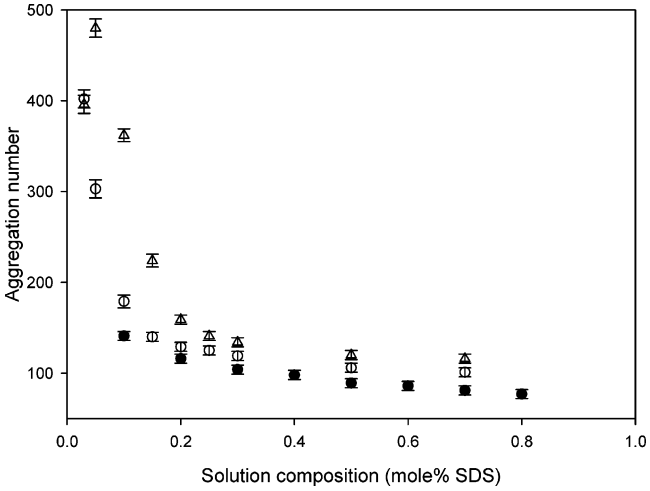

Figure 2. Variation in micelle aggregation number with solution composition for 25 mM SDS/$C_{12}E_6$: (●) in D_2O; (○) in 0.01 M NaCl; (△) in 0.05 M NaCl.

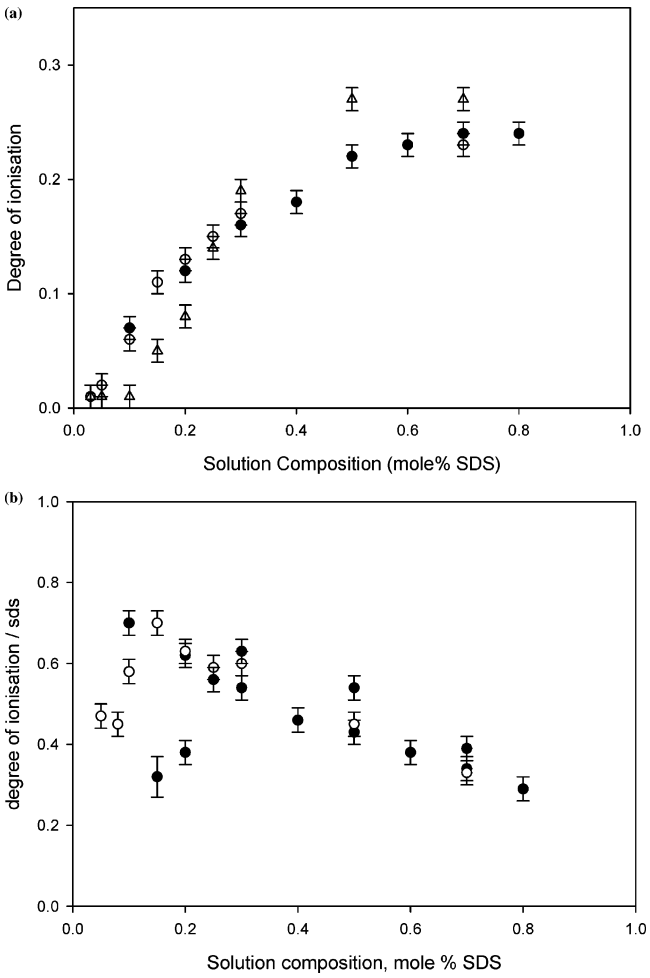

Figure 3. (a) Degree of ionization for 25 mM SDS/$C_{12}E_6$ micelles as a function of solution composition: (●) in D_2O; (○) in 0.01 M NaCl, (△) in 0.05 M NaCl. (b) Same as part a except degree of ionization/SDS molecule in the SDS/$C_{12}E_6$ micelles.

consistent with significant intermicellar interactions, even for the nonionic rich micelles. In electrolyte, the scattering is markedly different, even at the lowest amount of added electrolyte of 0.01 M NaCl.

For the solutions rich in SDS, there is still a significant suppression of the scattering at low *Q*, indicative of the presence of pronounced intermicellar interactions. It is less pronounced at the higher electrolyte concentration (0.05 M NaCl) and for the solutions richer in the nonionic surfactant (see Figure 1b and c). For the solutions most rich in the nonionic surfactant, there is no interaction maximum in the data, and the scattering is now consistent with substantial micellar growth. The solid lines in the figures are model fits to the data using the procedure,

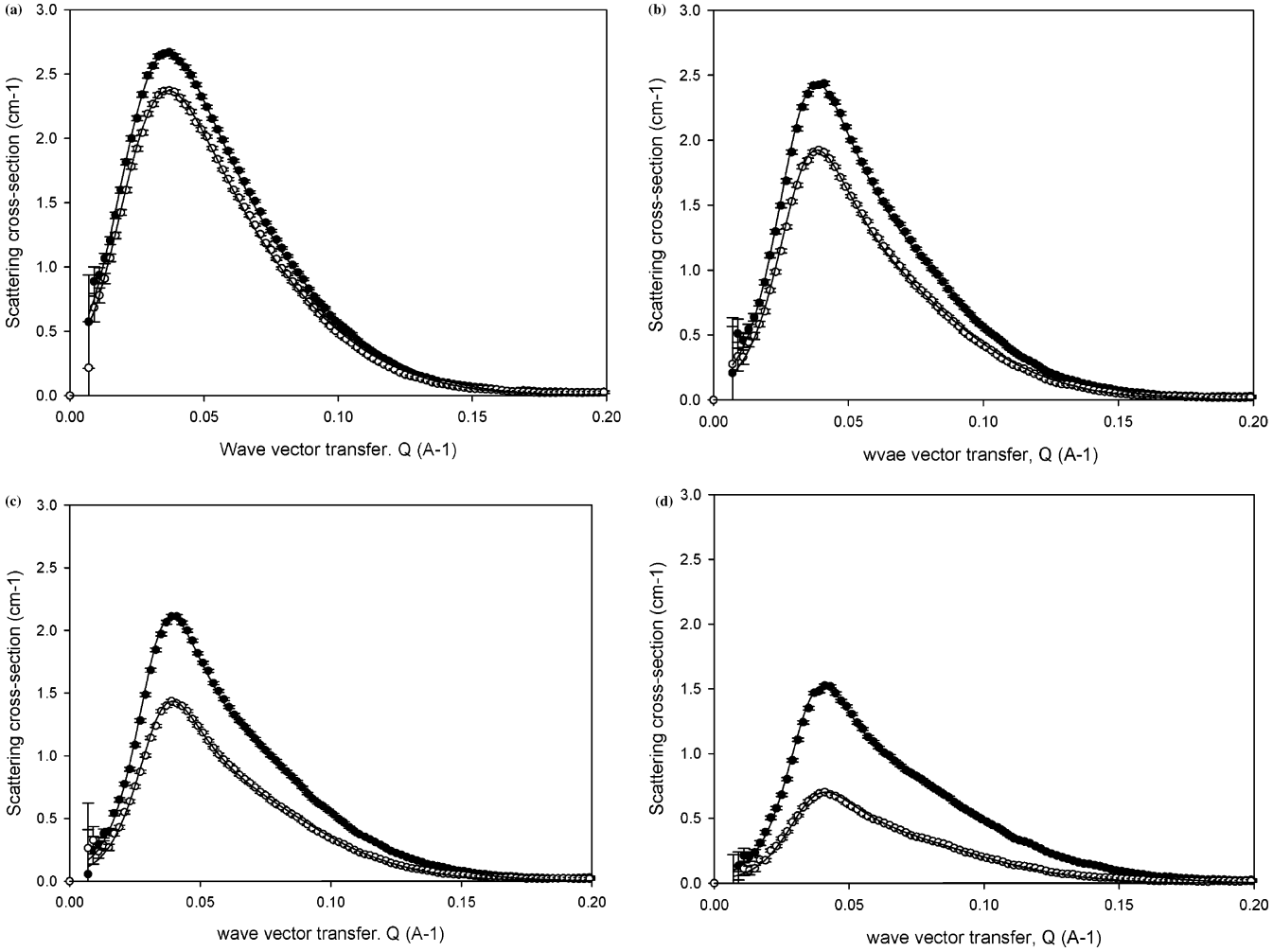

Figure 4. Scattered intensity for 25 mM SDS/$C_{12}E_8$ in D_2O [(○) *h*-SDS/*h*-$C_{12}E_8$; (●) *d*-SDS/*h*-$C_{12}E_8$]: (a) 10/90 mole ratio SDS/$C_{12}E_8$; (b) 20/80; (c) 30/70; (d) 50/50. The solid lines are model calculations as described in the text and using the parameters in Table 4.

model, and constraints described in the Experimental Section (eqs 2 and 3). The key model parameters are summarized in Table 2.

The variation in aggregation number with solution composition is shown in Figure 2 for the SDS/$C_{12}E_6$ mixtures. In D_2O, in the absence of electrolyte, and for solutions rich in SDS, the micelles are consistent with relatively small globular micelles and also consistent with previously reported values.[47,50] With increasing nonionic content, modest micellar growth is observed, eventually leading to values of the aggregation number that are similar to that for pure $C_{12}E_6$ micelles.[52]

With the addition of electrolyte (0.01 and 0.05 M NaCl), the micelles show an increase in aggregation number for the SDS rich solutions, again consistent with previous observations.[47] For the nonionic rich solutions (>80 mol % $C_{12}E_6$), there is a more marked increase in the aggregation number for the increasingly nonionic rich compositions. For added NaCl at 0.05 M, there is a maximum in the aggregation number at a composition of ~95 mol % $C_{12}E_6$, qualitatively consistent with previously reported observations.[41,42]

Table 3 shows the degree of ionization (δ, where $\delta = z/v$) for the SDS/$C_{12}E_6$ mixed micelles, and the degrees of ionization/SDS molecule (δ_s) are plotted as a function of composition in Figure 3.

The degree of ionization increases with increasing SDS composition and reaches a plateau value which is similar in the presence and absence of electrolyte. For solutions rich in nonionic surfactant, this effective degree of ionization is negligibly small. Plotting the degree of ionization/SDS molecule in the micelles (see Figure 3b) shows a rather different behavior. The degree of ionization/SDS is now highest for the nonionic rich micelles and shows a rather different dependence on the solution composition which is dependent upon the amount of added electrolyte.

3.2. SDS/$C_{12}E_8$. Figure 4 shows the small angle scattering from the SDS/$C_{12}E_8$ mixed micelles in D_2O. In D_2O, the measurements were made for the two isotopic combinations of *h*-SDS/*h*-$C_{12}E_8$ and *d*-SDS/*h*-$C_{12}E_8$. Figure 4 shows the evolution of the scattering from both isotopic combinations in the solution composition range from 10/90 to 50/50 mole ratio SDS/$C_{12}E_8$. The data are consistent with globular micelles, with a strong intermicellar interaction, which is more pronounced for the solutions richer in SDS.

The data for the isotopic combination *h*-SDS/*h*-$C_{12}E_8$ arise from the entire micelle, whereas for the isotopic combination *d*-SDS/*h*-$C_{12}E_8$ the SDS is effectively "index matched" to the D_2O solvent and the scattering arises only from the $C_{12}E_8$ component of the mixed micelles. This results in the lower scattered intensity for the *d*-SDS/*h*-$C_{12}E_6$ combination but a variation with scattering vector which is similar to that for *h*-SDS/*h*-$C_{12}E_6$, reflecting the change in composition and indicative of no overall change in the micelle structure. From the ratio of the scattering data for the two isotopic combinations (see eq 4), the micelle composition can be evaluated directly.

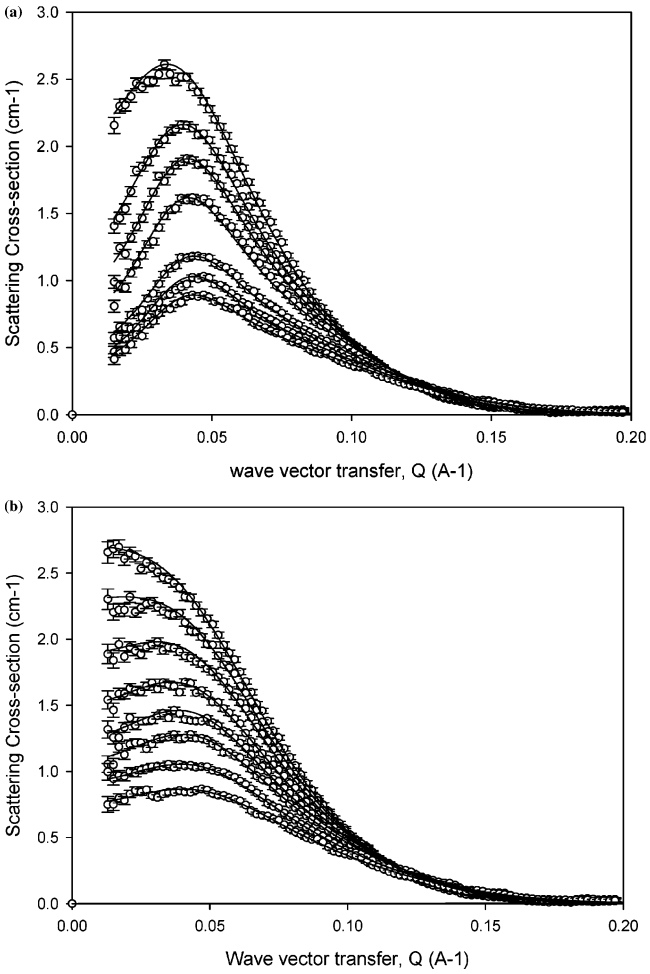

Figure 5. Scattered intensity for 25 mM SDS/$C_{12}E_8$ (a) in 0.01 M NaCl and (b) in 0.05 M NaCl for different solution compositions: (a) from bottom curve to top curve, 60/40, 50/50, 40/60, 30/70, 20/80, and 10/90; (b) from bottom curve to top curve, 80/20, 70/30, 60/40, 40/60, 30/70, 20/80, and 10/90. The solid lines are model calculations as described in the text and using the parameters in Table 4.

As expected from regular solution theory (RST), at this concentration (25 mM), the micelle compositions are close to the solution composition. These measurements were made in order to make that confirmation, and the solution composition is subsequently used as a constraint in the modeling of the micelle structure; that is, the micelle compositions were fixed at the solution composition. In Figure 4, the increasing difference in the scattering arising from the two isotopic combinations is hence merely reflecting the change in composition, from 10/90 to 50/50 mole ratio SDS/$C_{12}E_8$. Figure 5 shows the equivalent SANS data for the SDS/$C_{12}E_8$ mixture in 0.01 M NaCl and 0.05 M NaCl/D_2O, where in this case only the isotopic combination *h*-SDS/*h*-$C_{12}E_8$ (as for SDS/$C_{12}E_6$) in D_2O was measured. The scattering data for the solutions in electrolyte show the same broad trends as observed for SDS/$C_{12}E_6$.

In electrolyte, the trend with composition is similar to SDS/$C_{12}E_6$, except that with increasing electrolyte and nonionic content the suppression of the scattering at low Q (which arises as a consequence of the intermicellar interactions) is less pronounced. This is consistent with a reduction in the intermicellar interactions (that is, the compressibility, $\sim 1/S(0)$, is not so large), and in 0.05 M NaCl, there is almost no evidence of pronounced interactions. In marked contrast to the data for SDS/$C_{12}E_6$ in electrolyte, there is no evidence from the data for a more pronounced micellar growth for solutions rich in $C_{12}E_8$.

TABLE 4: Model Parameters for SDS/$C_{12}E_8$ Mixed Micelles at a Concentration of 25 mM[a]

solution composition (mole % SDS), isotopic combination	ν	z	R_2 (Å)	e	f
(a) In D_2O					
10/90 *hh*	115	8.0	23.4	1.92	0.96
dh	112	8.0	23.4	1.88	0.91
20/80 *hh*	102	13.0	22.3	1.71	1.01
dh	102	13.0	23.3	1.70	1.07
30/70 *hh*	90	16.0	23.1	1.5	0.91
dh	89	16.0	23.1	1.5	1.01
40/60 *hh*	83	18.5	22.8	1.39	0.94
dh	82	18.5	22.8	1.39	1.11
50/50 *hh*	79	20.0	22.5	1.3	0.97
dh	78	20.0	22.5	1.3	1.17
60/40 *hh*	78	21.0	21.9	1.3	0.95
dh	74	21.0	21.9	1.24	0.94
(b) In 0.01 M NaCl					
10/90	121	10.3	23.6	2.03	1.03
20/80	106	15.0	23.4	1.77	1.03
30/70	97	18.6	23.2	1.63	1.0
40/60	91	19.7	22.9	1.52	1.04
60/40	80	21.8	22.3	1.34	1.02
70/30	81	23.4	21.9	1.36	1.05
80/20	81	23.2	21.3	1.36	0.98
(c) In 0.05 M NaCl					
10/90	118	13.3	23.6	1.98	1.04
20/80	113	15.6	23.4	1.89	1.06
30/70	107	19.5	23.2	1.79	1.03
40/60	100	24.1	22.9	1.69	1.02
50/50	96	28.8	22.6	1.62	0.99
60/40	92	29.8	22.3	1.53	0.98
70/30	91	26.5	22.3	1.52	0.98
80/20	90	26.5	21.3	1.50	0.95

[a] In part a, κ varied over the composition range from 0.0094 to 0.028 Å^{-1} and $R_1 = 16.7$ Å; in part b, κ varied over the composition range from 0.033 to 0.042 Å^{-1}; and in part c, κ varied over the composition range from 0.072 to 0.075 Å^{-1}.

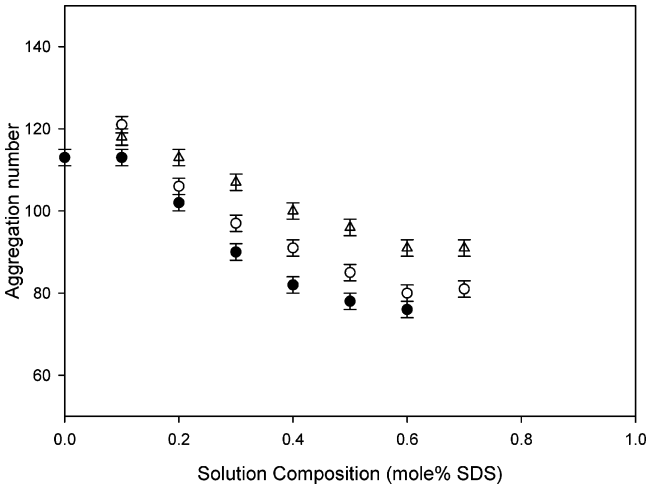

Figure 6. Variation in micelle aggregation number with solution composition for 25 mM SDS/$C_{12}E_8$: (●) in D_2O; (○) in 0.01 M NaCl; (△) in 0.05 M NaCl.

The solid lines in Figures 4 and 5 are model fits to the data, using the model and procedure previously described. The key model parameters are summarized in Table 4.

The variation of the micelle aggregation number with solution composition is shown in Figure 6 for the SDS/$C_{12}E_8$ mixture.

In D_2O, in the absence of electrolyte, and for SDS rich solution compositions, the micelles are relatively small globular micelles, consistent with that expected for SDS.[47,50] With added electrolyte, modest micelle growth is observed, as previously

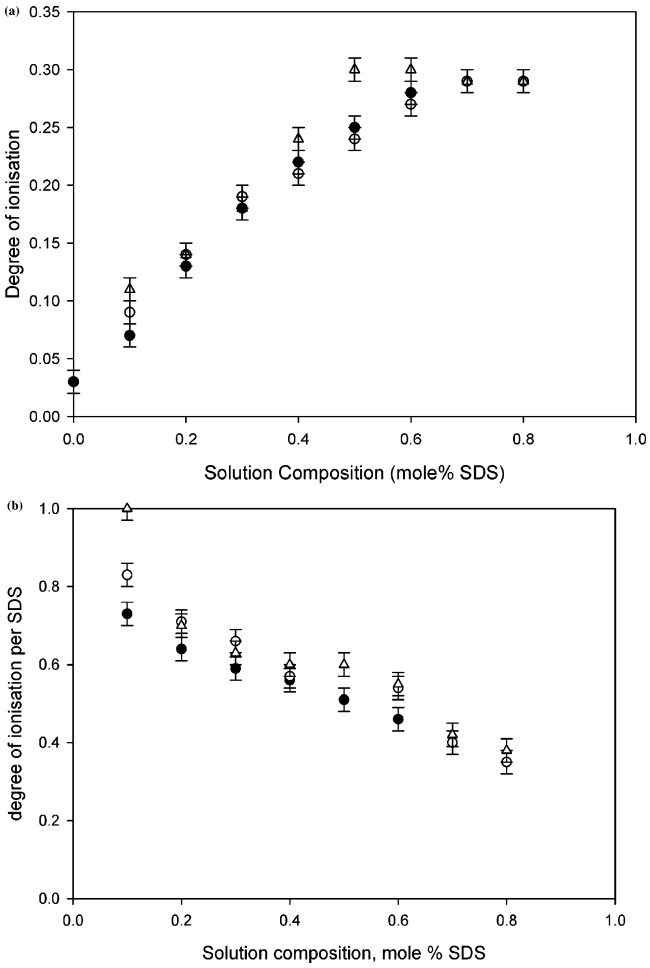

Figure 7. Same as Figure 3 except for 25 mM SDS/$C_{12}E_8$.

TABLE 5: SDS/$C_{12}E_8$ Mixed Micelles: Degree of Ionization

solution composition	in D_2O		in 0.01 M NaCl		in 0.05 M NaCl	
(mole % SDS)	δ	δ(per SDS)	δ	δ(per SDS)	δ	δ(per SDS)
10/90	0.07	0.73	0.09	0.83	0.11	1.0
20/80	0.13	0.64	0.14	0.71	0.14	0.7
30/70	0.18	0.59	0.19	0.66	0.18	0.63
40/60	0.22	0.56	0.21	0.56	0.24	0.6
50/50	0.25	0.51			0.30	0.6
60/40	0.28	0.46	0.27	0.55	0.32	0.55
70/30			0.29	0.40	0.29	0.42
80/20			0.29	0.35	0.29	0.38

reported elsewhere.[47] With increasingly nonionic rich solutions, there is now only modest micellar growth, and at the most nonionic rich solution compositions, the micelles are consistent with those expected for pure $C_{12}E_8$ micelles[52] and are still relatively small globular micelles. Furthermore, as the solutions become richer in nonionic surfactant, electrolyte has a progressively smaller impact, in marked contrast to what is observed for the SDS/$C_{12}E_6$ mixtures.

Table 5 shows the degree of ionization and the degree of ionization/SDS molecule for the SDS/$C_{12}E_8$ mixtures, and the data are plotted as a function of solution composition in Figure 7.

The variation in the degree of ionization of the micelles with solution composition shows the same general behavior as observed for the SDS/$C_{12}E_6$ mixtures. The prominent differences are that for the SDS/$C_{12}E_8$ mixture the degree of ionization in the limit of SDS rich solutions is higher than that for the SDS/$C_{12}E_6$ mixtures. Furthermore, the behavior is essentially independent of electrolyte concentration. The degree of ionization/SDS molecule shows a rather different behavior (see Figure 7b) from that observed for SDS/$C_{12}E_6$. Although the general trend is for the degree of ionization/SDS molecule to increase with increasing nonionic content, it does not go through a maximum as observed for SDS/$C_{12}E_6$.

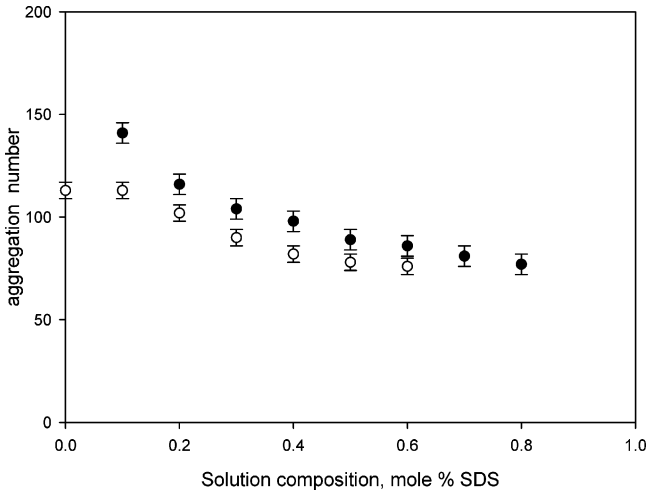

Figure 8. Micelle aggregation number for SDS/nonionic mixed micelles in D_2O as a function of solution composition: (●) SDS/$C_{12}E_6$; (○) SDS/$C_{12}E_8$.

4. Discussion

The mixed SDS/nonionic micelles in D_2O show a modest growth from relatively small globular micelles for SDS rich solution compositions to somewhat larger elliptical micelles for nonionic rich compositions. This general behavior is observed for both nonionic surfactants, $C_{12}E_6$ and $C_{12}E_8$. At the extremes of the composition range (either SDS or nonionic rich), the micelle aggregation number is consistent with that expected for SDS,[47] for $C_{12}E_6$,[51,52] and for $C_{12}E_8$ [52] micelles. Comparing directly SDS/$C_{12}E_6$ and SDS/$C_{12}E_8$ (see Figure 8), the aggregation numbers for SDS rich solutions are similar for both mixtures as expected, but the micellar growth for nonionic rich compositions is more pronounced for SDS/$C_{12}E_6$.

This is consistent with simple packing arguments,[11] which would imply that the $C_{12}E_8$ (with its larger headgroup volume and hence area) would promote smaller and more highly curved aggregates than $C_{12}E_6$. This is also entirely consistent with a change of the headgroup steric contribution to the free energy of micellization, as predicted by Blankschtein et al.[42] The results of Garamus,[43] measured for SDS/$C_{12}E_6$/D_2O but at a temperature (15 °C) rather close to the Krafft temperature of the SDS, are also broadly consistent with those presented here for SDS/$C_{12}E_6$ in D_2O. The results for SDS rich solutions are comparable, whereas the results from this study (at 25 °C) show a more pronounced growth for the increasingly nonionic rich compositions. Although the measurements were made at a temperature well removed from the cloud temperature of $C_{12}E_6$ (~45 °C[53]), in this concentration regime, some micellar growth is expected with increasing temperature.[54] For $C_{12}E_8$, the cloud temperature is relatively much higher, ~80 °C.[53] In the presence of low concentrations of electrolyte (0.01 and 0.05 M NaCl), the variation in aggregation number with solution composition is now markedly different to that in D_2O, and furthermore, there is a marked difference between the behavior of the two ionic/nonionic mixtures, SDS/$C_{12}E_6$ and SDS/$C_{12}E_8$ (see Figures 2 and 6). For the mixture SDS/$C_{12}E_8$ (see Figure 6), the variation is less pronounced for the solutions most rich in nonionic

surfactant, and added electrolyte has a relatively larger effect on the SDS rich solutions. This is consistent with electrolyte screening the charge on the SDS molecules and promoting micellar growth.[47] Although added electrolyte will also affect the nonionic surfactant, the effects are expected to be relatively small for $C_{12}E_8$. Added electrolyte will reduce the cmc and reduce the clouding temperature,[52] and this was attributed primarily to a reduction in the alkyl chain solubility by Carale et al.[55] At these electrolyte concentrations, the effects will not be significant for $C_{12}E_8$. With added electrolyte, the mixed SDS/$C_{12}E_6$ micelles show a substantial increase in aggregation number for the solutions most rich in $C_{12}E_6$ (see Figure 2). In 0.05 M NaCl, the aggregation number reaches a maximum at a solution composition of ~95 mol % $C_{12}E_6$, consistent qualitatively with previous observations for SDS/$C_{12}E_6$[41,42] and for SDS/β-dodecyl maltoside mixtures.[31] These results and those previously reported for SDS/$C_{12}E_6$[41,42] suggest that the maximum, which has been rationalized as arising from a balance between the headgroup steric and electrostatic contributions to the free energy of micellization,[42,56] is extremely sensitive to those relative contributions. This was further demonstrated by Zoeller et al.[56] where the interplay between the steric and electrostatic interactions was investigated in dodecyl ethoxy sulfate micelles, and it was demonstrated that the effect of electrolyte on the micelle aggregation number was shifted to higher concentrations for larger ethoxy groups. By changing the ethoxy group, it was possible to tune the steric interaction relative to the electrostatic contribution. Such issues are in part responsible for the interesting trends with composition, electrolyte, and ethoxylate headgroup size. Clearly, the SDS/$C_{12}E_6$ mixture is more sensitive in the nonionic rich composition range ($\geq$70 mol % nonionic) than in the case for SDS/$C_{12}E_8$. This would imply that the steric and electrostatic contributions are more delicately balanced and can be more effectively perturbed in favor of micellar growth than in the case of SDS/$C_{12}E_8$. Alternatively, for the SDS/$C_{12}E_6$ mixture, the closer proximity of the clouding transition may have an impact, and it is well-known that added "salting out" electrolyte (NaCl) reduces the clouding temperature. However, at these amounts of added NaCl, the effects are expected to be minimal.[55,57]

The surface charge on the micelles, expressed here as the micelle ionization, $\delta = z/v$, shows a variation with solution composition and added electrolyte consistent with other observations;[31,38,43] see Figures 3 and 7. For solutions rich in nonionic surfactant, the surface charge is negligible, and it increases to a plateau value, 0.25−0.3, for solutions rich in SDS. This limiting value for SDS rich solutions is consistent with that reported for pure SDS micelles[47,50] and with the theoretical predictions of the "dressed micelle" model.[58] Consistent with those observations, an increase of electrolyte concentration results in only a modest change in δ. The degree of ionization shows a rather different dependence on the solution composition when plotted as the degree of ionization/SDS molecule in the mixed micelle (see Figures 3b and 7b). For SDS/$C_{12}E_8$, the degree of ionization decreases linearly with increasing SDS composition, and for the nonionic rich compositions, the SDS molecules are almost fully dissociated. A similar trend is observed in the SDS/$C_{12}E_6$ mixtures in D_2O and in the presence of electrolyte for solutions rich in SDS. However, in 0.01 and 0.05 M NaCl, the degree of ionization/SDS molecule goes through a maximum for solutions richer in the nonionic surfactant. This coincides with the composition region where the significant growth is observed (30 mol % SDS in 0.05 M NaCl and 15 mol % SDS in 0.01 M NaCl). In the next paragraph, we consider specifically the headgroup steric and electrostatic contributions to the free energy of micellization.

The differences in the variation of the aggregation number with composition and added electrolyte observed for SDS/$C_{12}E_6$ and for SDS/$C_{12}E_8$ potentially highlight the relative importance of the headgroup steric and electrostatic contributions to the free energy of micellization. Following the molecular thermodynamic approach of Blankschtein for mixed anionic/nonionic surfactant mixtures,[12−14] we have estimated the steric and electrostatic contributions, where

$$g_{\text{ster}}^{\text{mix}} = -kT\left[\alpha \ln\left(1 - \frac{a_{\text{ha}}}{a}\right) + (1-\alpha)\ln\left(1 - \frac{a_{\text{hb}}}{a}\right)\right] \quad (7)$$

where a_{ha} and a_{hb} are the headgroup cross-sectional areas of the two components, a is the area/surfactant molecule at the interface, and α is the surfactant mole ratio (estimates of $g_{\text{ster}}^{\text{mix}}$ for SDS/$C_{12}E_6$ and for SDS/$C_{12}E_8$ are made using $a \sim 59$, $a_{\text{SDS}} \sim 25$, $a_{\text{c12e6}} \sim 42$, and $a_{\text{c12e8}} \sim 52$ Å^2), and

$$g_{\text{elec}}^{\text{mix}} = \alpha^2 g_{\text{elec}}^{\text{a}} \pm 2\alpha(1-\alpha)(g_{\text{elec}}^{\text{a}} g_{\text{elec}}^{\text{b}})^{1/2} + (1-\alpha)^2 g_{\text{elec}}^{\text{b}} \quad (8)$$

which for a nonionic/ionic mixture reduces to

$$g_{\text{elec}}^{\text{mix}} = \alpha^2 g_{\text{elec}}^{\text{a}} \quad (9)$$

An approximate expression for $g_{\text{elec}}^{\text{a}}$ is taken from Nagarajan et al.[59]

$$g_{\text{elec}}^{\text{a}} = \frac{2\pi e^2 d}{\epsilon a_{\text{e}}}(1/1 + \kappa_0 l_{\text{c}}) \quad (10)$$

where l_{c} is the extended alkyl chain length (16.7 Å for C_{12}), d is equivalent to capacitor thickness in the double layer model (taken here to be ~4 Å), a_{e} is the equilibrium area/molecule (~58 Å^2), and κ is the inverse Debye screening length. Figure 9a shows the estimated variation in $g_{\text{ster}}^{\text{mix}}$ and $g_{\text{elec}}^{\text{mix}}$ for SDS/$C_{12}E_6$ and SDS/$C_{12}E_8$ as a function of solution composition and ionic strength.

Figure 9b shows the variation in the total contribution arising from the headgroup steric and electrostatic interactions to the free energy of micellization for both SDS/$C_{12}E_6$ and SDS/$C_{12}E_8$. The main contribution to the free energy of micellization is the large negative contribution from the transfer of the surfactant hydrocarbon chain from its unfavorable aqueous environment to the hydrocarbon micellar core, and it is typically ~18−19 kT.[12] The positive headgroup contributions are in contrast much smaller, but nevertheless important, and are typically ~2−4 kT. For solutions rich in nonionic surfactant, the headgroup free energy contribution is dominated by the steric term. In contrast, for solutions rich in SDS and especially in the absence of electrolyte, the electrostatic contribution dominates the headgroup free energy. When the electrolyte concentration is $\leq$0.05 M NaCl, and even for relatively SDS rich solutions, the steric and electrostatic contributions are comparable. For the SDS/$C_{12}E_8$ mixture, the variation in the total headgroup contribution with composition does not vary greatly with added electrolyte; the variation with composition is greater the lower the electrolyte concentration. This is entirely consistent with the observed variation in aggregation number with composition, where the largest variation is observed in the absence of electrolyte. For the SDS/$C_{12}E_6$ mixture, the steric hindrance of the EO_6 headgroup compared with the EO_8 headgroup is significantly less, whereas the electrostatic contributions are assumed to be similar. Hence, there is a more profound variation in the total

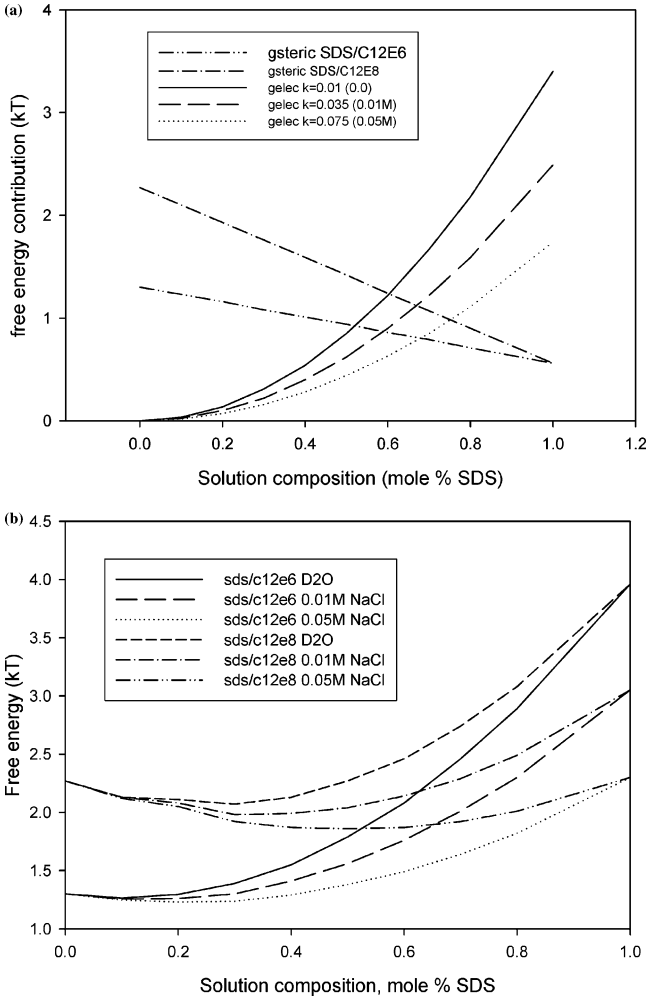

Figure 9. Calculated contributions to the free energy of micellization for SDS/$C_{12}E_6$ and SDS/$C_{12}E_8$ as a function of solution composition: (a) steric and electrostatic contributions; (b) total contribution (see figure for annotation).

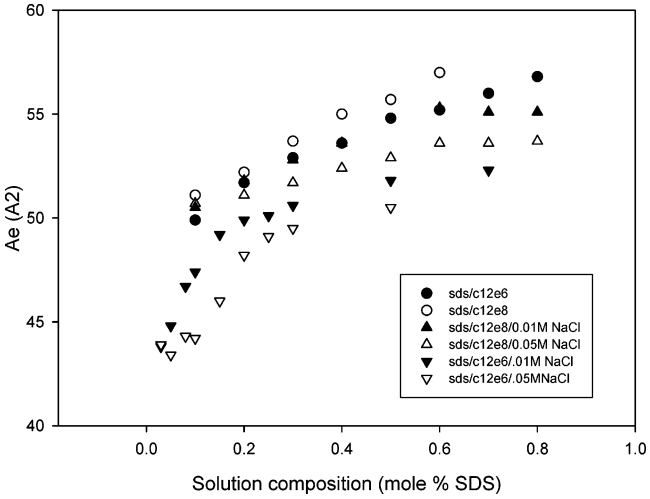

Figure 10. Variation of the "effective" area/molecule (Ae) with solution composition for SDS/$C_{12}E_6$ and SDS/$C_{12}E_8$ in D_2O, 0.01 M NaCl, and 0.05 M NaCl (see figure for annotation).

headgroup free energy contribution with solution composition. Except for the solution compositions most rich in SDS, over most of the composition range, this free energy contribution is significantly smaller for SDS/$C_{12}E_6$ than for SDS/$C_{12}E_8$. This is consistent with the generally larger micellar aggregation numbers for the SDS/$C_{12}E_6$ mixture and the more significant increase for solutions rich in nonionic surfactant. The total free energy contribution does show a weak minimum (in 0.05 M NaCl) in the composition regime where a maximum in the aggregation number is observed. The significance of this has been discussed extensively elsewhere.[41−43] However, given the uncertainty in the parameters in the model (eqs 7−10) and the approximations involved, the composition at which the minimum occurs can be manipulated. For example, for the SDS/$C_{12}E_8$ mixture, a minimum is observed for solutions relatively rich in SDS in 0.05 M NaCl, but there is no corresponding maximum in the micelle aggregation number. A relatively minor adjustment of the parameters in eq 7 will result in a substantial change in the occurrence of that minimum.

Although the free energy calculations do qualitatively explain most of the trends in the data, they do not fully account for the significant micellar growth for the nonionic rich SDS/$C_{12}E_6$ mixtures in 0.01 and 0.05 M NaCl. This behavior is highlighted in Figure 10 where the "effective" area/surfactant molecule is plotted as a function of solution composition for SDS/$C_{12}E_6$ and SDS/$C_{12}E_8$ in D_2O and in electrolyte.

From Nagarajan,[59] the aggregation number can be written as

$$v = \left(\frac{4\pi l_c^3}{3V_0}\right)\left(\frac{a_e l_c - 2}{V_0}\right)^{-1} \tag{11}$$

where V_0 is the volume per alkyl chain. From the known values of l_c (16.7 Å) and V_0 (350 Å^3) and the measured values of v (from Tables 1 and 2), a_e can be estimated. For most of the solutions, a_e decreases from ∼58 to ∼50 Å^2 for increasingly nonionic rich solutions. However, for SDS/$C_{12}E_6$ in 0.01 and 0.05 M NaCl, the onset of significant micellar growth for a nonionic rich solution, at ∼20 mol % SDS, is associated with an abrupt change in a_e. Values of a_e in the range 50−60 Å^2 are consistent with the elliptical micelles observed (the limiting value for spheres for a C_{12} alkyl chain is ∼65 Å^2), whereas the smaller values (<50 Å^2) are consistent with highly elongated micelles.

Although the general features are adequately explained qualitatively by the simple free energy arguments, the more significant growth of the SDS/$C_{12}E_6$ micelles for the nonionic rich solution compositions in electrolyte is not fully explained. This would imply that there is an electrolyte dependent contribution to the headgroup steric free energy of the ethylene oxide headgroups. Carale et al.[55] considered the effect of salt on intramicellar interactions and on micellization in nonionic surfactants and concluded that the most pronounced effect was on the solubility of the alkyl chain. Although a more refined calculation of the ethylene oxide chain steric contribution was made, where the chainlike nature of the headgroup was considered rather than its more approximate treatment as a hard sphere (as was originally used[12] and implied in the calculations made in this paper), no variation in aggregation with electrolyte concentration is predicted, and hence, broadly similar results to those in the absence of electrolyte were obtained.

In previous studies[61] on the interfacial mixing of SDS/maltoside surfactant mixtures, the enthalpic contribution to the nonideal free energy of mixing was recognized but not quantified in detail. A recent calorimetric study of the temperature dependence of the formation of mixed ionic/nonionic micelles by Golub and de Keizer[62] has demonstrated the importance of hydration to the enthalpy of mixed micelle formation. They showed for SDS/$C_{12}E_6$ mixed micelles that the differential enthalpy of mixed micelle formation (ΔH_{exc}) strongly depended upon temperature and the micelle composition at the nonionic

rich end of the composition range. This strong temperature dependence of the excess enthalpy is not attributable to headgroup electrostatic interactions, as discussed earlier. The temperature dependence is most pronounced for the nonionic rich compositions where the electrostatic interactions have only a minor effect and are largely independent of temperature. Hence, it was attributed to the increase in the hydrophobicity of the micelle headgroup region due to the dehydration of the EO chain caused by the presence of the ionic headgroups. With increasing ionic content, the electrostatic repulsion between the headgroups will depress the effect. This is akin to the reduction of the nonionic clouding temperature due to the addition of electrolyte. Hence, we can, as postulated in the previous paragraph and following the work of Golub and de Keizer,[62] attribute the sensitivity of the composition induced changes in micellar size with added electrolyte to changes in the enthalpy of micellization due to partial dehydration of the EO headgroups. The addition of small amounts of SDS induces that dehydration, which is further enhanced by the addition of electrolyte. The addition of further SDS increases the headgroup repulsion, resulting in an increased hydration due to a greater exposure of the headgroups to the solvent phase, and hence minimizing the effects of dehydration. This is qualitatively consistent with our observations for SDS/$C_{12}E_6$. For the SDS/$C_{12}E_8$ mixture, the larger headgroup size and correspondingly larger hydration is consistent with the observed reduction in sensitivity. Indeed, the cloud point for $C_{12}E_8$ is immeasurably large, and the effect of electrolyte, correspondingly smaller.

In their original study on SDS/$C_{12}E_6$ mixtures, Blankschtein et al.[42] reported that their molecular thermodynamic calculations for pure $C_{12}E_6$ micelles are extremely sensitive to the value of a_e used. It is clear from Figure 10 that there is an abrupt change in a_e at the point at which significant micellar growth occurs. Hence, it is concluded that the electrolyte induced growth for the nonionic rich micelles in SDS/$C_{12}E_6$ is associated with the $C_{12}E_6$ being very close to the sphere−rod transition[60] under these conditions and that subtle changes in the ethylene oxide conformation and hydration will initiate that transition.

5. Summary

In the anionic/nonionic mixed surfactant micelles of SDS/$C_{12}E_6$ and SDS/$C_{12}E_8$, changing the nonionic surfactant headgroup geometry and the addition of electrolyte have demonstrated the sensitivity of the micelle structure, aggregation number, and surface charge to electrostatic and steric contributions in the surfactant headgroup region. Due to the relatively large steric contribution, the SDS/$C_{12}E_8$ mixed micelles show relatively modest growth with composition and added electrolyte. In contrast, the SDS/$C_{12}E_6$ micelles exhibit a more pronounced growth, and in this mixture, the delicate balance of the headgroup free energy contributions is illustrated by the substantial micellar growth for nonionic rich compositions in modest electrolyte concentrations.

References and Notes

(1) Shiloach, A.; Blankschtein, D. *Langmuir* **1998**, *14*, 7166.

(2) Scamehorn, J. F. In *Mixed Surfactant Systems*; Ogino, K., Abe, M., Eds.; Marcel Dekker: New York, 1992.

(3) Rosen, M. In *Phenomena in mixed surfactant systems*; Scamehorn, J. F., Ed.; ACS Symp Ser no 311; American Chemical Society: Washington, DC, 1988.

(4) Rubingh, D. N. In *Solution chemistry of surfactants*; Mittal, K. L., Ed.; Plenum Press: New York, 1979; Vol. 1.

(5) Holland, P. M. *Colloids Surf., A* **1986**, *19*, 171.

(6) Hines, J. *Curr. Opin. Colloid Interface Sci.* **2001**, *6*, 350.

(7) Zoeller, N.; Shiloach, A.; Blankschtein, D. *Curr. Opin. Colloid Interface Sci.* **1997**, *2*, 294.

(8) Nagarajan, R.; Ruckenstein, E. *Langmuir* **1991**, *7*, 2934.

(9) Naor, A.; Puvvada, S.; Blankschtein, D. *J. Phys. Chem.* **1992**, *96*, 7830.

(10) Tanford, C. *J. Phys. Chem.* **1972**, *76*, 3020.

(11) Isrealachivili, J. N.; Mitchell, D. J.; Ninham, B. W. *J. Chem. Soc., Faraday Trans. 2* **1976**, *72*, 1525.

(12) Puvvada, S.; Blankschtein, D. *J. Phys. Chem.* **1992**, *96*, 5567.

(13) Shiloach, A.; Blankschtein, D. *Langmuir* **1998**, *14*, 1618.

(14) Shiloach, A.; Blankschtein, D. *Langmuir* **1997**, *13*, 3968.

(15) Nagarajan, R. *Langmuir* **1985**, *1*, 331.

(16) Bergstrom, M.; Eriksson, J. C. *Langmuir* **2000**, *16*, 7173.

(17) Hines, J. D. *Langmuir* **2000**, *16*, 7575.

(18) Mulqueen, M.; Blankschtein, D. *Langmuir* **1999**, *15*, 8832.

(19) Penfold, J. Neutron scattering studies of micellar structure. *Encyclopedia of Surf. and Coll. Sci.*; Academic Press: Amsterdam, 2002; p 3653.

(20) Cabane, B. In *Surfactant Solutions*; Zana, R., Ed.; Surfactant Science Series 22; Marcel Dekker: New York, 1987.

(21) Candau, S. J. In *Surfactant Solutions*; Zana, R., Ed.; Surfactant Science Series 22; Marcel Dekker: New York, 1987.

(22) Zana, R. In *Surfactant Solutions*; Zana, R., Ed.; Surfactant Science Series 22; Marcel Dekker: New York, 1987.

(23) Lindman, B.; Soderman, O.; Wennerstrom, H. In *Surfactant Solutions*; Zana, R., Ed.; Surfactant Science Series 22; Marcel Dekker: New York, 1987.

(24) Danino, D.; Gupta, R.; Satyavolu, J.; Talmon, Y. *J. Colloid Interface Sci.* **2002**, *249*, 180.

(25) Thomas, H. G.; Lomatin, A.; Blankschtein, D.; Benedek, G. *Langmuir* **1997**, *13*, 209.

(26) Bergstrom, M.; Pedersen, J. S. *Langmuir* **1999**, *15*, 2250.

(27) Misselyn-Baudin, A. M.; Thibaut, A.; Grandjean, J.; Broze, G.; Jerome, R. *Langmuir* **2000**, *16*, 4430.

(28) Zana, R.; Levy, H.; Danino, D.; Talmon, Y.; Kwetkat, K. *Langmuir* **1997**, *13*, 462.

(29) Griffiths, P. C.; Stilbs, P.; Paulsen, K.; Howe, A. M.; Pitt, A. R. *J. Phys. Chem. B* **1997**, *101*, 915.

(30) Griffiths, P. C.; Cheung, A. Y. F.; Finney, G. J.; Pitt, A. R.; Howe, A. M.; King, S. M.; Heenan, R. K.; Bales, B. L. *Langmuir* **2002**, *18*, 1065.

(31) Bucci, S.; Fagotti, C.; Degiorgio, V.; Piazza, R. *Langmuir* **1991**, *7*, 824.

(32) Garamus, V. *Langmuir* **1997**, *13*, 6388.

(33) Ruiz, C. C.; Aguiar, J. *Langmuir* **2000**, *16*, 7946.

(34) Douglas, C. B.; Kaler, E. W. *Langmuir* **1994**, *10*, 1075.

(35) Baglioni, P.; Rei, L.; Rivara-Miula, E.; Kevan, L. *J. Am. Chem. Soc.* **1993**, *115*, 4286.

(36) Ciccarelli, D.; Costantino, L.; D'Enrico, G.; Paduano, L.; Vitagliano, V. *Langmuir* **1998**, *14*, 7136.

(37) Gao, H. C.; Zhao, S.; Mao, S. Z.; Yuan, H. Z.; Yu, J. Y.; Shen, L. F.; Du, Y. R. *J. Colloid Interface Sci.* **2002**, *249*, 200.

(38) Griffiths, P. C.; Cheung, A. Y. F.; Farley, C.; Paul, A.; Heenan, R. K.; King, S. M.; Pettersson, E.; Stilbs, P.; Ranganathan, R. *J. Phys. Chem. B* **2004**, *108*, 1351.

(39) Penfold, J.; Staples, E.; Thompson, L.; Tucker, I.; Hines, J.; Lu, J. R.; Thomas, R. K. *Langmuir* **1995**, *11*, 2496.

(40) Penfold, J.; Staples, E.; Thompson, L.; Tucker, I.; Hines, J.; Thomas, R. K.; Lu, J. R.; Warren, N. *J. Phys. Chem. B* **1999**, *103*, 5204.

(41) Penfold, J.; Staples, E.; Tucker, I. *J. Phys. Chem. B* **2002**, *106*, 8891.

(42) Shiloach, A.; Blankschtein, D. *Langmuir* **1998**, *14*, 7166.

(43) Garamus, V. M. *Langmuir* **2003**, *19*, 7214.

(44) Heenan, R. K.; King, S. M.; Penfold, J. *J. Appl. Crystallogr.* **1997**, *30*, 1140.

(45) Heenan, R. K.; King, S. M.; Osborn, R.; Stanley, H. B. RAL Internal Report 1989, RAL-89-128.

(46) Lu, J. R.; Lee, E. M.; Thomas, R. K.; Penfold, J.; Flitsch, S. L. *Langmuir* **1993**, *9*, 1352.

(47) Hayter, J. B.; Penfold, J. *Colloid Polym. Sci.* **1983**, *261*, 1032.

(48) Hayter, J. B.; Penfold, J. *Mol. Phys.* **1981**, *42*, 109.

(49) Hayter, J. B.; Hansen, J. P. *Mol. Phys.* **1982**, *42*, 651.

(50) Griffiths, P. C.; Paul, A.; Heenan, R. K.; Penfold, J.; Ranganathan, R.; Bales, B. L. *J. Phys. Chem. B* **2004**, *108*, 3810.

(51) Zulauf, M.; Weckstrom, H.; Hayter, J. B.; Degiorgio, V.; Corti, M. *J. Phys. Chem.* **1985**, *89*, 3411.

(52) Penfold, J.; Staples, E.; Tucker, I.; Cummins, P. *J. Colloid Interface Sci.* **1997**, *185*, 424.

(53) van Os, N. M.; Haak, J. R.; Rupert, L. A. M. *Physicochemical properties of selected anionic, cationic and nonionic surfactants*; Elsevier: Amsterdam, 1993.

(54) Magid, L. J.; Triolo, R.; Johnson, J. S. *J. Phys. Chem.* **1984**, *88*, 3730.

(55) Carale, T. R.; Pham, Q. T.; Blankschtein, D. *Langmuir* **1994**, *10*, 109.
(56) Zoeller, N.; Blankschtein, D. *Langmuir* **1998**, *14*, 7155.
(57) Penfold, J.; Staples, E. J.; Tucker, I.; Cummins, P. G. *J. Colloid Interface Sci.* **1997**, *185*, 424.
(58) Hayter, J. B. *Langmuir* **1992**, *8*, 2873.
(59) Nagarjan, R. *Langmuir* **2002**, *18*, 31.
(60) Mazer, N. A.; Benedeck, G. B.; Carey, M. C. *J. Phys. Chem.* **1976**, *80*, 1075.
(61) Hines, J. D.; Garrett, P. R.; Rennie, G. K.; Thomas, R. K.; Penfold, J. *J. Phys. Chem. B* **1997**, *101*, 7121.
(62) Tatiana, P.; Golub, P.; de Keizer, A. *Langmuir* **2004**, *20*, 9506.